Molecular Architecture of SMC Proteins and the Yeast Cohesin Complex

Christian H. Haering,[1,4] Jan Löwe,[2,4]
Andreas Hochwagen,[1,5] and Kim Nasmyth[1,3]
[1]Research Institute of Molecular Pathology
Dr. Bohr Gasse 7
A-1030 Vienna
Austria
[2]MRC Laboratory of Molecular Biology
Hills Road
Cambridge CB2 2QH
United Kingdom

Summary

Sister chromatids are held together by the multisubunit cohesin complex, which contains two SMC (Smc1 and Smc3) and two non-SMC (Scc1 and Scc3) proteins. The crystal structure of a bacterial SMC "hinge" region along with EM studies and biochemical experiments on yeast Smc1 and Smc3 proteins show that SMC protamers fold up individually into rod-shaped molecules. A 45 nm long intramolecular coiled coil separates the hinge region from the ATPase-containing "head" domain. Smc1 and Smc3 bind to each other via heterotypic interactions between their hinges to form a V-shaped heterodimer. The two heads of the V-shaped dimer are connected by different ends of the cleavable Scc1 subunit. Cohesin therefore forms a large proteinaceous loop within which sister chromatids might be entrapped after DNA replication.

Introduction

When cells divide, not only must they duplicate all their chromosomes precisely but they must also segregate the two products, known as sister chromatids, to opposite poles of the cell prior to cytokinesis. Cohesion between sister chromatids has a crucial role during this process. It first enables cells to attach sister kinetochores to microtubules with opposing polarity (bi-orientation) and subsequently resists the tendency of these microtubules to pull chromatids toward opposite spindle poles (Nasmyth, 2001). An equilibrium between these two counteracting forces leads to the alignment of chromatid pairs on the metaphase plate. Finally, when all chromosomes have aligned on the spindle, the sudden destruction of cohesion triggers disjunction of chromatids and their traction toward opposite poles during anaphase.

Recent studies in the budding yeast *Saccharomyces cerevisiae* have identified five proteins that are essential for cohesion between sister chromatids: Scc1 (Mcd1), Scc3, Smc1, Smc3, and Pds5 (for review, see Nasmyth, 2001). Orthologs of all five proteins have been found in

other eukaryotes so far studied and several have also been implicated in sister chromatid cohesion (Losada et al., 1998; Pasierbek et al., 2001; Sonoda et al., 2001). Scc1, Scc3, Smc1, and Smc3 are subunits of a soluble protein complex, called cohesin (Losada et al., 1998; Sumara et al., 2000; Toth et al., 1999). Pds5 also associates with cohesin but appears to be less tightly bound than the other four subunits.

In yeast, most cohesin remains associated with chromosomes until metaphase but dissociates at the onset of anaphase, when cohesion is dissolved. This event is triggered by cleavage of cohesin's Scc1 subunit by a cysteine protease, called separase (Uhlmann et al., 1999, 2000). The bulk of cohesin in animal cells in contrast dissociates from chromatin during prophase/prometaphase in a separase-independent manner. Nevertheless, a residual amount of cohesin remains associated with chromosomes, in particular around centromeres, until metaphase. This fraction behaves like the bulk of yeast cohesin, in that its cleavage is necessary for sister chromatid separation at the onset of anaphase (Hauf et al., 2001; Waizenegger et al., 2000). Cleavage of cohesin's Scc1 subunit may therefore be a universal trigger for chromosome segregation.

Cohesin's Smc1 and Smc3 subunits are both members of the SMC (structural maintenance of chromosomes) family of proteins, which exist in virtually all organisms including both bacteria and archaea (Soppa, 2001). SMC proteins share a five-domain structure, with globular N- and C-terminal domains separated by a long (circa 100 nm or 900 residues) coiled coil segment in the center of which is a globular "hinge" domain. All SMC proteins appear to form dimers, either forming homodimers with themselves, as in the case of prokaryotic SMC proteins, or heterodimers between different but related SMC proteins, as in the case of cohesin, which contains an Smc1/Smc3 heterodimer (see below), and condensin, which contains an Smc2/Smc4 heterodimer (Hirano et al., 1997).

An electron microscopic study of bacterial SMC proteins has established that their coiled coils are antiparallel (Melby et al., 1998). This orientation brings the N- and C-terminal globular domains (from either different or identical protamers) together, which unites an ATP binding site (Walker A motif) within the N-terminal domain with a Walker B motif (DA box) within the C-terminal domain, to form a potentially functional ATPase of the ABC (ATP binding cassette) family (Hopfner et al., 2000; Löwe et al., 2001). The hinge domains of these bacterial SMC proteins are sufficiently flexible that the two head domains of a single homodimer can either be at opposite ends of a V-shaped molecule or in close juxtaposition of a stick-shaped one (Melby et al., 1998).

Despite these insights, it has never been established whether the two protamers of an SMC dimer contact each other along their entire length, as they would if the coiled coils were intermolecular, or whether they do so merely in the hinge region, as they would if the coiled coils were intramolecular. In the first case, the N- and C-terminal domains forming a head would be part of

[3]Correspondence: nasmyth@nt.imp.univie.ac.at
[4]These authors contributed equally to this work.
[5]Present address: Center for Cancer Research, Massachusetts Institute of Technology, Cambridge, Massachusetts 02139.

different molecules, whereas in the second, they would be the two ends of the same molecule (Figure 2A). This issue has a crucial bearing on how Smc1 and Smc3 interact within the cohesin complex and its resolution is essential for understanding the geometry not only of cohesin but also of condensin.

Much less is known about the structure of cohesin's other subunits. Scc1-like proteins are most conserved at their N and C termini. The two separase cleavage sites within yeast and mammalian Scc1 proteins are located in the center of the protein between these two conserved domains. Importantly, cleavage at either site is sufficient to destroy cohesion at the metaphase to anaphase transition (Buonomo et al., 2000; Hauf et al., 2001; Uhlmann et al., 1999). Meanwhile, Pds5 (Neuwald and Hirano, 2000; Panizza et al., 2000) and Scc3 (D. Barford, personal communication) orthologs consist largely of HEAT repeats or HEAT repeat-like structures, respectively.

If we are to understand how cohesin links DNA molecules together, it is essential to know how cohesin's non-SMC subunits interact with Smc1 and Smc3. But to achieve this, it is crucial to first establish the fundamental geometry of the Smc1/3 heterodimer. By studying the architecture of Smc1 and Smc3 and by solving the structure of an SMC hinge domain associated with short coiled coils from the bacterium *Thermotoga maritima*, we have established that the coiled coils of many if not most SMC proteins are in fact intramolecular. Cohesin therefore contains two long arms, one composed of Smc1 and the other of Smc3, which are connected at one end by heterotypic interactions between their hinge domains. The other two ends, containing the ABC-like ATPase, can be connected by Scc1, whose N- and C-terminal domains bind to Smc3's and Smc1's heads, respectively. This suggests a novel hypothesis for how cohesin associates with chromosomes and mediates cohesion between sisters. We suggest that Scc1-mediated closure of cohesin's arms after a DNA strand has been embraced creates a topological link between these partners.

Results

The SMC Hinge Domain Forms a Doughnut-Shaped Dimer with All N and C Termini Located on One Face

Biochemical experiments involving the head domains of eukaryotic SMCs are only interpretable when it is known if their antiparallel coiled coil segments are intra- or intermolecular, because this determines whether the heads are composed of N- and C-terminal domains from the same or different polypeptide chains (Figure 2A). At issue here is the mechanism by which SMC proteins dimerize. In an attempt to address this, we solved the crystal structure of the SMC hinge domain from the bacterium *Thermotoga maritima*. A fragment containing residues 485–670 (HTMC2) crystallized in two different crystal forms, containing either one or two homodimers. The hinge domain crystal structures (Figure 1) only reveal ordered residues from approximately 501 to 656. Residues 485 to 500 and 657 to 670 are invisible due to disorder, although they have been predicted to form a coiled coil. This is probably the case because the coiled

coil segments are too short to be stable. It is however clear that the hinge domains are stable in the absence of ordered coiled coil segments. A DALI (Holm and Sander, 1995) search revealed no close structural homologs in the Protein Data Bank.

The hinge domain monomer is composed of two domains (I and II) that are related by a pseudo-2-fold symmetry operation (Figure 1A). Domain I contains a short three-stranded β sheet flanked by two α helices whereas domain II contains a five-stranded β sheet also flanked by α helices. Inner helices (H4, H5, H9, and H10) are involved in domain I/domain II interactions whereas outer ones (H6 and H11) are involved in dimer interactions. Domains I and II are linked by a long but ordered loop. An important feature of the monomer is that the fold separates the N and C termini of the same chain by 22 Å. The hinge domain dimer is formed by combining the β sheets of two monomers into two eight-stranded β sheets (Figures 1B and 1C). This and the outer helices H6 and H11 are the only contacts holding the dimer together. It is worth noting that the first structure solved in spacegroup P2$_1$ contained a dimer in which one of the dimer contacts is disturbed by crystal contacts and the dimer has no true 2-fold axis. A second crystal form however contained dimers with true 2-fold symmetry (spacegroup P2$_1$2$_1$2$_1$), and we believe this is the biologically relevant conformation. The hinge dimer structure locates all N and C termini on one face of the doughnut-shaped structure. This explains EM pictures of SMC proteins where V-shaped or closed conformations seem favored (Anderson et al., 2002; Melby et al., 1998). The N and C termini from different monomers are closer together (13 Å) than the termini from the same monomer (22 Å). Nevertheless, both distances are compatible with the formation of coiled coils, leaving open whether the hinge seeds intra- or intermolecular coiled coils. The crystal structure of a protein fragment containing longer coiled coil segments eventually settled this issue (see below). We meanwhile turned our attention to cohesin's Smc1 and Smc3 proteins, where the anticipated heterotypic dimerization allowed us to address this issue in an independent manner.

Structure of Smc1/3 Heterodimers and Smc3 Monomers

To examine the structure formed by yeast cohesin SMC subunits, we first compared the hydrodynamic properties of Smc3 alone with that of complexes formed together with Smc1. We expressed Smc3 as an N-terminally His$_6$-tagged version either alone or together with Smc1 in insect cells. Both Smc3 and the Smc1/Smc3 complexes were found largely in the soluble cytosolic and nuclear fractions derived from the insect cell extracts. The proteins were partially purified over a nickel-affinity resin before determining Stokes radii and sedimentation coefficients by gel filtration and gradient centrifugation, respectively. This yielded Stokes radii of 8.0 nm for the Smc1/His$_6$Smc3 complex and 7.4 nm for His$_6$Smc3 alone (Figure 2B, left panels). Both the Smc1/His$_6$Smc3 complex and His$_6$Smc3 alone sedimented in sharp peaks in glycerol gradients, the former with a sedimentation velocity of 8.0S (which is similar to that of *Xenopus* Smc1/3 heterodimers) and the latter with 4.4S (Figure 2B, right panels).
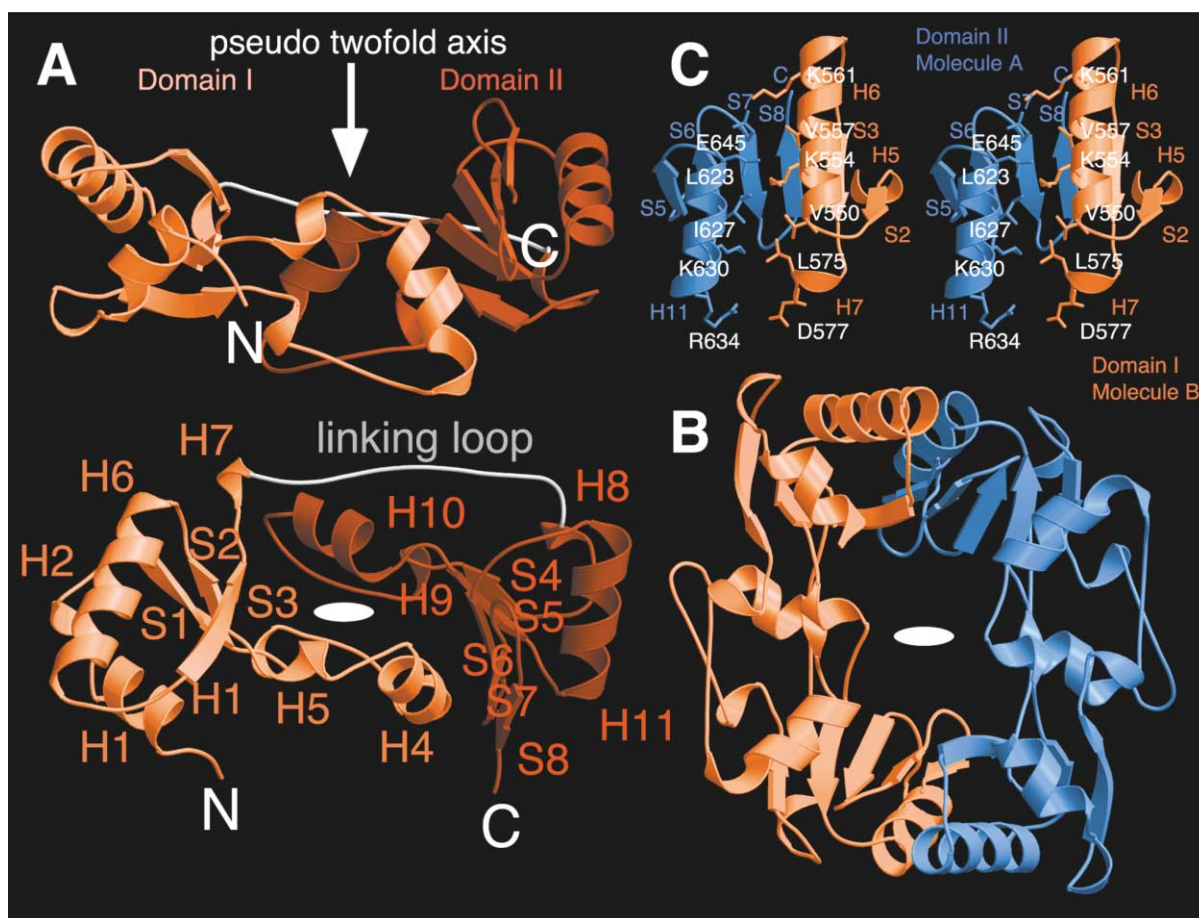
Figure 1. Crystal Structure of the Hinge Domain from *Thermotoga maritima* SMC Protein (Construct HTMC2, Residues 485-670)

(A) Ribbon plot of one subunit of the hinge dimer solved in spacegroup P2₁ at 2.1 Å, resolution by seleno-methionine substitution and MAD. Top and bottom view are rotated by 90° around the Y axis.

(B) The hinge dimer is a doughnut-shaped structure. The structure shown has been solved in spacegroup P2₁2₁2₁ at 3.0 Å resolution (twinning fraction 0.158) by molecular replacement using the P2₁ high-resolution structure as starting model.

(C) Stereo drawing of the dimer contact. The contact consists of an antiparallel β sheet contact of S3 and S8 and a helix/helix contact between H6 and H11. Residues highlighted are the only residues involved in the dimer contact. The corresponding residues in the yeast hinge domains of Smc1 and Smc3 would provide all specificity of hinge dimer formation. Figure prepared with MOLSCRIPT (Kraulis P.J., 1991).

The Stokes radii and sedimentation velocities were used to estimate native molecular weights using the method of Siegel and Monty (1966). This yielded a molecular weight of ~260 kDa for the Smc1/His₆Smc3 complex and ~130 kDa for His₆Smc3 alone, which is in good agreement with predicted molecular weights of 282 kDa for an (Smc1)₁/(Smc3)₁ heterodimer and 141 kDa for an Smc3 monomer. The large Stokes radii and low S values, relative to globular proteins of similar molecular weight, are typical for elongated proteins. The equal intensities of the Smc1 and His₆Smc3 bands after silver staining (Figure 2B) are also consistent with the Smc1/Smc3 complex being an equimolar heterodimer.

We next visualized the Smc1/3 heterodimer by electron microscopy after rotary shadowing. We obtained high-resolution images that closely resembled those from prokarotic SMCs, which included the different types of conformation seen for *E. coli* MukB and *B. subtilis* SMC proteins (Melby et al., 1998). The majority of molecules had an "open V" or "Y" shaped conformation, in which the terminal head domains lie apart and the coiled coil arms are either separated over their whole or only part of their length, respectively (Figure 2C). Some molecules showed kinks in their coiled coils, which might be an important feature to create the flexibility of the SMC arms. The Smc1/3 heterodimer also adopted the "coils spread" conformation, in which the head domains lie close together but the arms have bowed apart (Figure 2C). With a total arm length of ~65 nm, consisting of a ~45 nm coiled coil stretch and head and hinge domains of about 10 nm diameter, the overall dimensions of the Smc1/3 heterodimer are similar to those of prokarotic SMCs. In contrast to a recent electron microscopy study on human and frog cohesin complexes (Anderson et al., 2002), yeast Smc1/3 heterodimers in the open V conformation had the arms separated at an average angle of only 35°, and angles of more than 60° were very rare. The similarity of the Stokes radii of Smc3 monomers and Smc1/3 heterodimers (Figure 2B) also suggests that the two arms of the latter are rarely wide open.

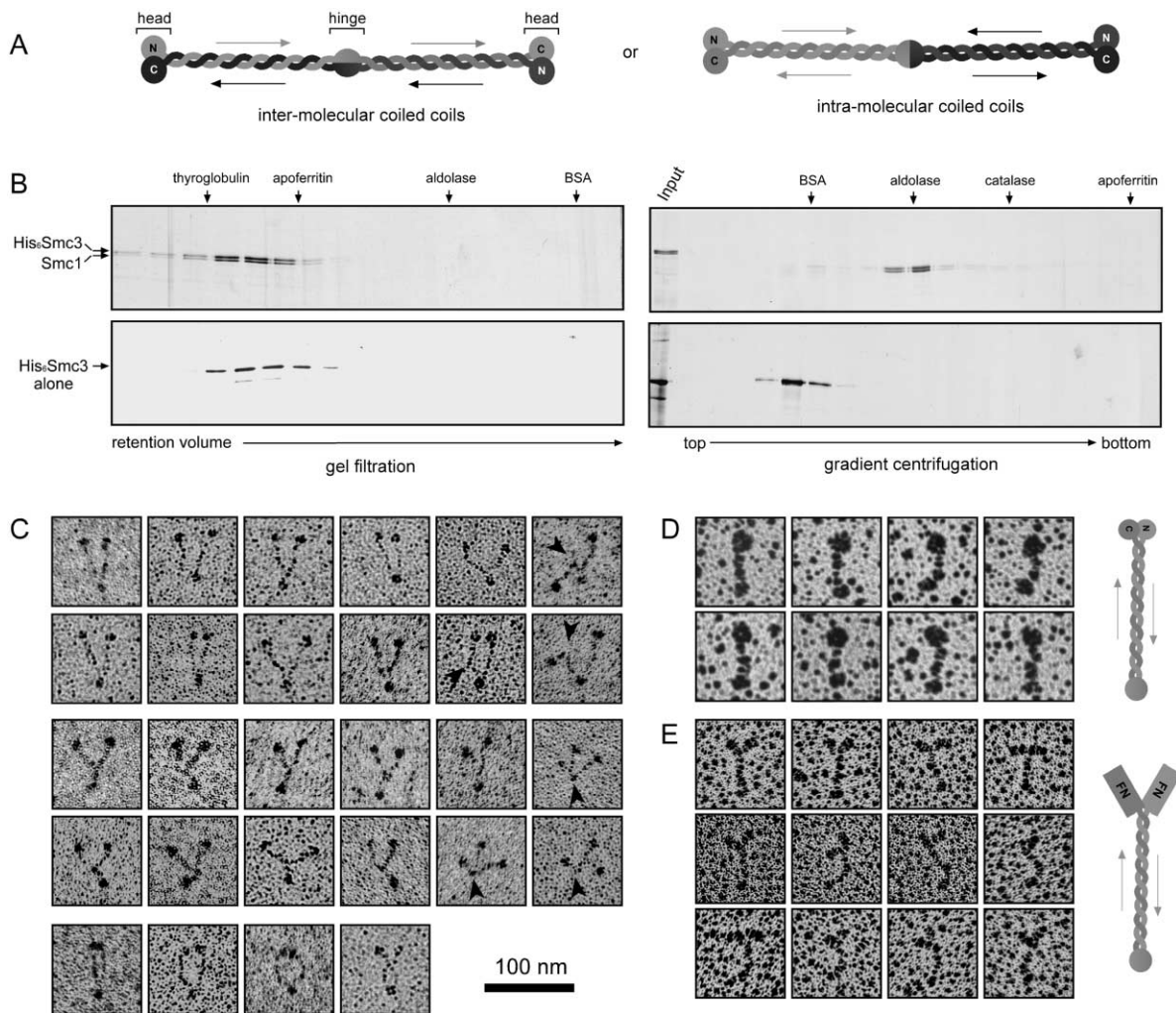These images, as well as those from prokaryotic

Figure 2. Smc1 and Smc3 Form a V-Shaped 1:1 Heterodimer with Intramolecular Coiled Coils

(A) Two possible models of SMC dimerization.

(B) Hydrodynamic properties of the Smc1/3 heterodimer and of the Smc3 monomer. Smc1 coexpressed with His$_6$Smc3 or His$_6$Smc3 expressed alone in insect cells were partially purified over Ni^{2+}-NTA. Imidazole eluates were run on a Sephacryl HR300 gel filtration column or on a glycerol gradient centrifugation. Proteins in gel filtration elution fractions (left panels) or in the fractionated gradient (right panels) were detected by silver staining after SDS-PAGE.

(C) Electron micrographs of the Smc1/His$_6$Smc3 heterodimer. The Smc1/3 heterodimer from the gel filtration peak fraction was visualized in the electron microscope after rotary shadowing with a 1 nm platinum layer. Upper two rows, open V conformation; middle two rows, Y conformation; lower row, coils spread conformation. Arrows show kinks in the coiled coil arms (bar = 100 nm).

(D) Electron micrographs of the Smc3 monomer. The His$_6$Smc3 monomer from the gel filtration peak fraction was visualized in the electron microscope after rotary shadowing with a 2 nm platinum layer.

(E) Electron micrographs of chimeric fibronectin-Smc3 monomers. N- and C-terminal globular domains of His$_6$Smc3 were replaced by thick fibronectin segments and purified by Ni^{2+}- NTA and gel filtration. The purified monomers were rotary shadowed with a 1 nm platinum layer.

SMCs, are consistent with both intra- and intermolecular coiled coils (Figure 2A). These two alternatives nevertheless make very different predictions as to the behavior and properties of single Smc1 or Smc3 protamers. If their coiled coils were intramolecular, then individual SMCs should form stable rod-shaped monomers containing a single coiled coil, with the hinge domain at one end and the globular head containing both N- and C-terminal domains at the other. These monomeric rods would be equivalent to one arm of the heterodimer. If on the other hand they were intermolecular, then the two amphipathic α helices of a single SMC protamer

would lack their dimerization partner. They might therefore no longer form a coiled coil and might instead adopt a disorganized structure with a propensity to aggregate.

The properties of Smc3 when expressed alone suggest that it forms intramolecular coiled coils: Smc3 is soluble in the absence of Smc1 and sediments with a discrete 4.4S sedimentation velocity (Figure 2B). The same is true for Smc1 (data not shown). Under the electron microscope, we observed rod-like structures (65–70 nm in length) with a large globular domain at one end and a smaller one at the other (Figure 2D). Most molecules had this configuration, which presumably corre-

sponds to the Smc3 arm of the heterodimer, with the larger globular domain containing Smc3's N- and C-terminal domains. To confirm this interpretation, we replaced Smc3's terminal domains by the 6-10 repeats from fibronectin, which can be identified as a short thick rod in electron micrographs (Melby et al., 1998). As expected, this resulted in replacement of the larger terminal globular domain by a pair of short rods with the dimensions expected for the fibronectin repeats (Figure 2E).

SMC Heterodimerization Is Conferred Solely by Hinge Domains

While bacterial genomes usually encode only a single SMC-like protein, eukaryotic ones encode at least six different members (Soppa, 2001), which invariably act in pairs. Smc1 interacts with Smc3 in cohesin while Smc2 interacts with Smc4 in condensin. If SMC proteins form intramolecular coiled coils, then the specificities of their pairwise interactions should be conferred solely by their hinge domains. A series of experiments in which we either removed or swapped hinge domains imply that possession of heterotypic hinges is both necessary and sufficient for the interaction between Smc1 and Smc3. A version of Smc1 whose hinge domain was replaced by a short peptide linker (Smc1Δhinge) failed to bind Smc3 (Figure 3A). While Smc3 cannot bind to a differently tagged version of the same protein (Figure 3B, top panel), a chimeric version of Smc3 whose hinge (and hinge alone) had been replaced by that of Smc1 (Smc3hinge1) bound to Smc3 (Figure 3B, top panel) but not to Smc1 (Figure 3B, middle panel). Finally, a chimeric version of Smc1 with an Smc3 hinge did not bind to Smc3 itself but bound to Smc3 containing Smc1's hinge (Figure 3B, bottom panel). Remarkably, the complex formed between Smc3 and the chimeric Smc3hinge1, which only contains coiled coil sequences from Smc3, eluted from a gel filtration column at an identical position to that of Smc1/3 dimers (not shown) and adopted a similar set of structures when viewed by electron microscopy, including the open V-shaped conformation (Figure 3C). This last result is easy to explain if the Smc1/3 heterodimer's coiled coils were intramolecular but difficult if they were intermolecular.

Even when expressed alone, Smc3's hinge domain but neither its N- nor C-terminal domains bound to Smc1 with an efficiency similar to that of intact Smc3 (Figure 3D). In contrast, Smc3's hinge domain failed to bind the chimeric Smc1 molecule with a hinge derived from Smc3. If interaction between heterotypic hinges were the sole means by which Smc1 and Smc3 were held together, then the affinity of an isolated Smc3 hinge for Smc1 might be expected to be similar to that of intact Smc3 protein. To investigate this, we used BIAcore solid state affinity measurements to estimate on rate (k_a), off rate (k_d), and affinity ($K_A = k_a/k_d$) constants by measuring the on and off rates of Smc1 binding to immobilized intact Smc3 or Smc3 hinge alone at different concentrations (Figure 3E). The off rates of Smc3 and its hinge alone were very similar and correspond to a half-life of ~25 min, whereas the on rate of Smc3 was about twice that of its hinge. This difference could easily be due to steric factors, namely, the hinge may be more accessible

to Smc1 when situated at the end of a long coil than when more closely bound to the BIAcore matrix. The calculated affinity constants for both types of molecules are around ~2×10^8/M^{-1}, indicative of a very strong interaction. These data imply that Smc3's coiled coil region makes little or no contribution to its Smc1 binding affinity, which is consistent with the coiled coils being intra- and not intermolecular.

SMC Molecules Form Intramolecular Coiled Coils

To reexamine whether the bacterial SMCs also form intramolecular coiled coils, we attempted crystallization of *T. maritima* SMC hinge domain fragments containing longer adjacent coiled coil sequences. Only one such construct (aa 473-685, HTMC9) produced crystals. To obtain an unbiased view, the structure was resolved with independent phases using seleno-methionine substituted protein and MAD at 3.0 Å resolution in space-group C2 (Figure 3F). Again, the crystals contain exclusively dimers. The core dimer of the hinge domain is essentially the same as described in Figure 1. However, this time coiled coil segments are clearly visible. The helices are, as expected, antiparallel but they originate from the same chain, which implies that *T. maritima*'s SMC contains intramolecular coiled coils. A properly scaled model of SMC proteins resulting from the above studies and earlier structural work on the head domains (Löwe et al., 2001) is shown in Figure 3G. Several conclusions follow from this general architecture. The hinge dimer is the only part of the structure holding the more than 100 nm long SMC dimer together. Only a few residues in the hinge dimer interface (Figure 1C) contribute to this interaction. Second, the intramolecular coiled coil ensures that the head domains are composed of N- and C-terminal domains from a single SMC chain, as predicted by our biochemical experiments with yeast Smc1 and Smc3. Our structure is therefore consistent with the notion that one of cohesin's heads is composed of N- and C-terminal domains from Smc1 while the other is composed of N- and C-terminal domains from Smc3.

Scc1 Binds to the Head Domains of Smc1 and Smc3

Having established the geometry of Smc1/3 heterodimers, we next investigated how they interact with cohesin's other subunits. We first tested whether Scc1 binds to the Smc1/3 heterodimer. Both the heterodimer and individual Smc1 and Smc3 monomers bound efficiently to Scc1 when coexpressed in insect cells (Figures 4A and 4D). The heterodimer furthermore copurified in a complex with Scc1 in a gel filtration column (Figure 4B). The only major contaminant was a Hsp70 chaperone protein, which was found to be associated with baculovirus expressed Scc1 previously (Uhlmann et al., 2000). Replacement of Smc1's hinge domain with a short peptide linker had little or no effect on its ability to bind Scc1 (Figure 4C). In contrast, removal of both head domains from the Smc1/3 heterodimer abolished its ability to bind Scc1, even though the headless SMCs bound to each other efficiently to form a soluble complex (Figure 4D). To test whether Smc3's head alone is sufficient to bind Scc1, we created an artificial head in which Smc3's N-terminal domain was connected to its C-terminal domain by a short peptide linker. This isolated
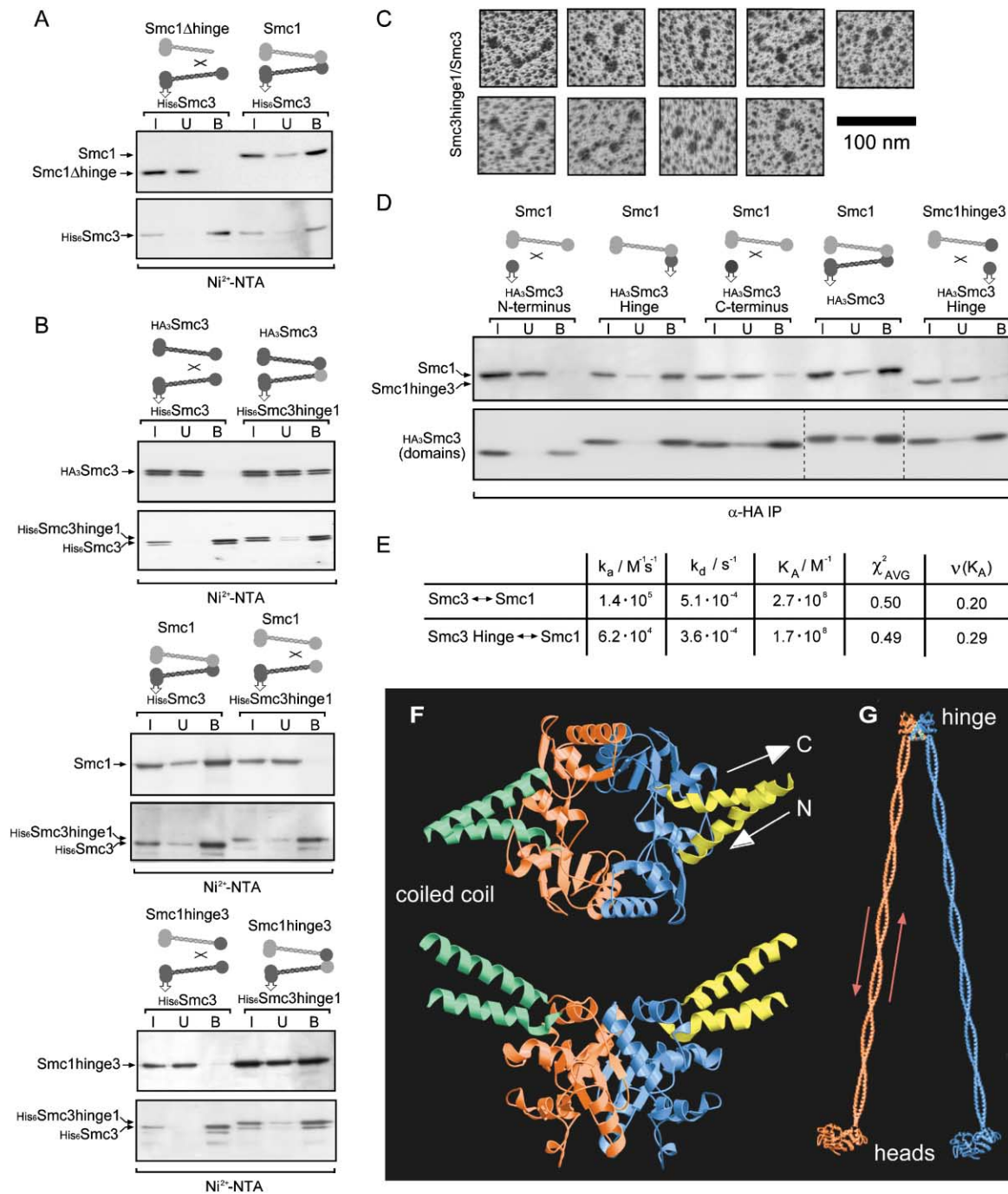
Figure 3. Smc1/3 Dimerization Specificity Is Solely Conferred by the Hinge Domains

(A) The hinge domain is necessary for Smc1/3 dimerization. Smc1Δhinge or Smc1 were coexpressed with His$_6$Smc3 in insect cells and subjected to a pull-down assay on Ni^{2+}-NTA. The presence of Smc1Δhinge or Smc1 in input (I), unbound (U), and bound (B) fractions was probed by immunoblotting with an antibody specific to the N terminus of Smc1 (upper panel) and the efficiency of Smc3 binding to the resin with anti-His antibody (lower panel).

(B) Only molecules with opposite hinge domains can dimerize. Smc1, HA$_3$Smc3, or Smc1hinge3 were coexpressed in insect cells with either His$_6$Smc3 or His$_6$Smc3hinge1, and protein association of each combination was assayed as in (A).

(C) Electron micrographs of the Smc3hinge1/Smc3 dimer. The His$_6$Smc3hinge1/ HA$_3$Smc3 dimer was purified from insect cells over Ni^{2+}-NTA and gel filtration. Proteins in the peak fraction from the gel filtration were rotary shadowed with a 2 nm platinum layer and visualized in the electron microscope.

(D) The hinge domain of Smc3 is sufficient for binding to Smc1. N-terminal, hinge, and C-terminal globular domains of Smc3 were coexpressed with Smc1 in insect cells as HA$_3$-tagged proteins. The globular domains were immunoprecipitated and their ability to pull down Smc1 was tested by immunoblotting for Smc1 (upper panel). Full-length HA$_3$Smc3 was used as a positive control. In addition, the association of the HA$_3$Smc3hinge domain with Smc1hinge3 was tested. In all experiments, the efficiency of the HA$_3$-immunoprecipitation was tested by blotting against the HA$_3$ epitope (lower panel).

Smc3 head bound Scc1 efficiently (Figure 4E). Addition of short stretches of the coiled coil normally attached to this head did not augment Scc1's association with Smc3's head (data not shown).

N- and C-Terminal Scc1 Cleavage Fragments Bind to Smc3 and Smc1 Heads, Respectively

Scc1's cleavage by separase is necessary and sufficient to destroy sister chromatid cohesion. To shed light on the molecular mechanism of this crucial step, we next investigated the ability of Scc1's N- and C-terminal cleavage fragments to bind Smc1 and Smc3. To do this, we created recombinant baculoviruses that express either an N-terminal Scc1 fragment, from the N terminus to the first separase cleavage site (aa 1-180), or a C-terminal Scc1 fragment, from the second separase cleavage site to the C terminus (aa 269-566), tagged with six histidine residues. Remarkably, both bound to the Smc1/3 heterodimer when coexpressed with Smc1 and Smc3 (data not shown). When Smc1 or Smc3 separately were coexpressed with the Scc1 fragments, Smc1 bound weakly to the N-terminal but strongly to the C-terminal cleavage fragment, while Smc3 only bound to the N-terminal but not to the C-terminal fragment (see Supplemental Figure S1 at http://www.molecule.org/cgi/content/full/9/4/773/DC1). Coimmunoprecipitation of Smc1 with Scc1's C-terminal cleavage fragment has also been detected in yeast extracts (Rao et al., 2001).

Together with the finding that intact Scc1 binds to the heterodimer's head domains, these data suggest that Scc1's N- and C-terminal fragments bind to Smc3's and Smc1's head domains, respectively. To test this, we coexpressed each Scc1 fragment with heterodimers lacking both heads, lacking only that of Smc1, or lacking only that of Smc3. As predicted, Smc1/3 dimers lacking both heads bound neither N- nor C-terminal Scc1 fragment, Smc1/3 dimers missing only Smc1's head bound Scc1's N-terminal but not its C-terminal fragment, whereas Smc1/3 dimers missing only Smc3's head bound Scc1's C-terminal but not N-terminal fragment (Figure 5A). The weak binding of Scc1's N-terminal fragment to Smc1 (Supplemental Figure S1 at http://www.molecule.org/cgi/content/full/9/4/773/DC1) is presumably due to an interaction with its exposed hinge domain, because this association is abolished when Smc1's hinge is attached to a headless Smc3 (Figure 5A) or to

an isolated Smc3 hinge domain (Supplemental Figure S1 at http://www.molecule.org/cgi/content/full/9/4/773/DC1), or when Smc1's hinge is replaced by that of Smc3 (data not shown). In all cases, the binding to the C-terminal fragment is maintained.

Though these results demonstrate that Scc1 possesses two different binding sites for separate heads of the Smc1/3 heterodimer, they do not address whether a single Scc1 molecule can bind to Smc1 and Smc3 heads simultaneously. If this occurs, then monomeric Scc1 should be able to link Smc1 and Smc3 together independently of any interaction between their hinges. We therefore investigated whether Scc1 can join Smc1 with the Smc3 chimera containing Smc1's hinge (Smc3hinge1). These two SMC proteins possess Smc1 and Smc3 head domains, respectively, but cannot bind to each other because they have homotypic hinges. They nevertheless copurified when coexpressed with intact Scc1 (Figure 5B, top). Likewise, Smc3 can be coprecipitated with Smc1 containing Smc3's hinge if these two proteins are coexpressed with intact Scc1, but not when coexpressed with Scc1's N- and C-terminal cleavage fragments (Figure 5B, bottom). Because other experiments (see below) suggest that Scc1 cannot link Smc1 and Smc3 heads by virtue of its own multimerization, we conclude that a single Scc1 molecule can bind simultaneously to the head domains of Smc1 and Smc3 and thereby form a bridge between them.

Most Cohesin Complexes in Yeast Contain Only a Single Smc1/3 Heterodimer

The presence of two independent SMC interaction sites within Scc1, one binding to Smc1's head and the other to that of Smc3, gives rise to two possibilities. Scc1 could link Smc1 and Smc3 heads either from the same heterodimer or from two different ones. To address this issue, we created a diploid yeast strain in which one Smc3 gene was tagged with the myc_{18} epitope and the other with the HA_6 epitope. Micrococcal nuclease digestion was used to release cohesin from chromatin (Ciosk et al., 2000), which had previously been separated from a "soluble" cell fraction (Liang and Stillman, 1997; Uhlmann et al., 1999). We immunoprecipitated $Smc3HA_6$ from both soluble and "chromatin released" fractions and used Western blotting to measure coprecipitation of $Smc3myc_{18}$ (Figure 6A). Little or no $Smc3myc_{18}$ was

---

(E) The Smc3hinge domain binds Smc1 as tightly as the full-length Smc3 protein does. HA_3Smc3 or the HA_3Smc3hinge domain produced in insect cells was bound to a CM5 sensor chip on the BIAcore system via a monoclonal anti-HA antibody attached to covalently linked anti-mouse Fc γ-specific antibody. Insect cell extracts containing defined concentrations of Smc1 as the ligand (five dilutions, ranging from 20 nM to 200 nM) were floated over the bound analytes, and association and dissociation kinetics were recorded. For each dilution, the data were fitted using a 1:1 Langmuir binding model with drifting baseline and corrected for unspecific binding to uninfected insect cell extracts. The average association and dissociation rate constants (k_a and k_d, respectively) are displayed and used to calculate the equilibrium binding constant (K_A). Low average values of χ^2 indicate the accuracy of the fit and the suitability of the 1:1 binding model, the variation coefficients ν for the binding constants show the consistency of the measurements over the ligand dilution range.

(F) Crystal structure of the hinge domain from *Thermotoga maritima* SMC protein (construct HTMC9, residues 473-685). Ribbon drawing of the hinge domain dimer, showing two stretches of antiparallel coiled coil (yellow and green). The orientation is essentially the same as in Figure 1B. The coiled coil segments are formed by residues from the same chain, resulting in an intramolecular coiled coil arrangement for SMC proteins. The structure shown was re-solved in spacegroup C2 by seleno-methionine substitution and MAD at 3.0 Å resolution.

(G) Architecture of SMC proteins. The intramolecular coiled coil results in the two arms being formed by separate chains with the hinge domains holding the two arms together. The coiled coil segments have been modeled using standard geometry and the crystal structures of the hinge and head domains have been described here and elsewhere (Löwe et al., 2001). Figure prepared using MOLSCRIPT (Kraulis P.J., 1991).
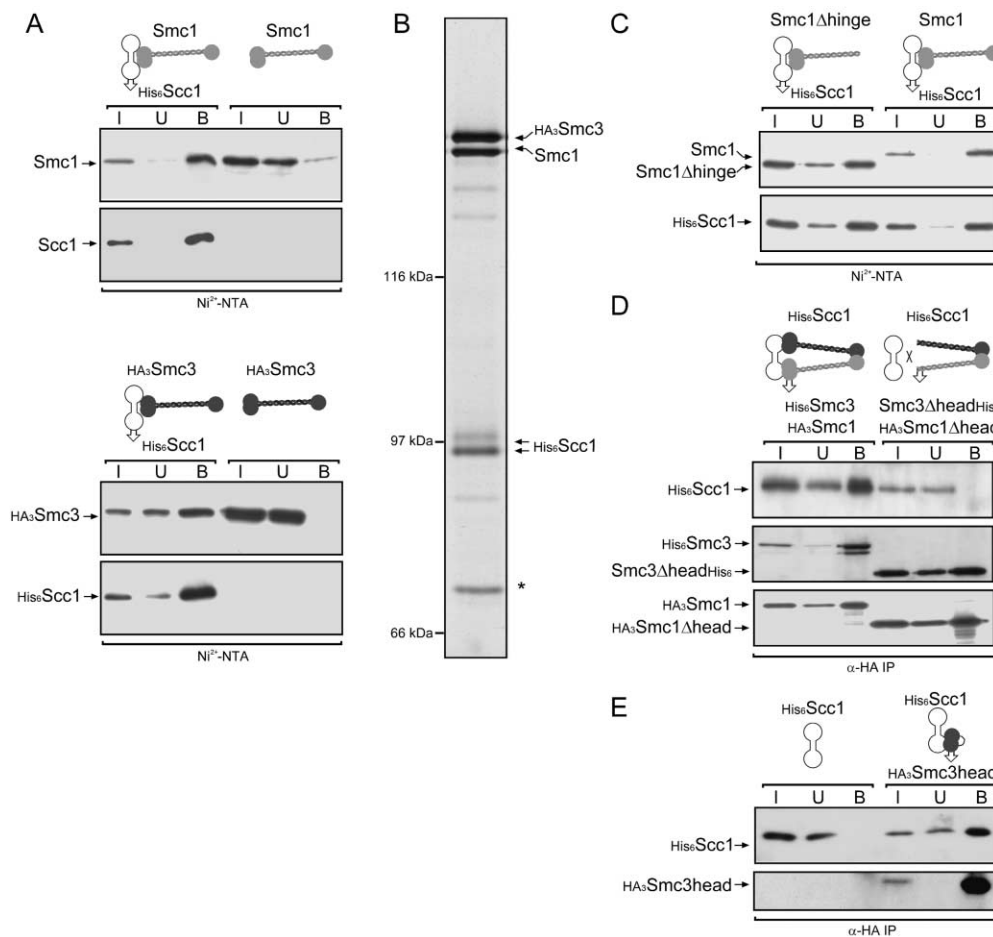
Figure 4. Smc1 and Smc3 Bind to Scc1 via Their Head Domains

(A) Smc1 and Smc3 individually bind to Scc1. Smc1 and HA$_3$Smc3 were expressed separately or coexpressed with His$_6$Scc1 in insect cells. Protein extracts were subjected to a pull-down assay on Ni^{2+}-NTA. The presence of Smc1 or Smc3 in input (I), unbound (U), and imidazol-eluate (bound, B) fractions was probed with anti-Smc1 or anti-HA specific antibodies on immunoblots, the efficient binding of His$_6$Scc1 to the resin is shown by probing with anti-His antibody.

(B) Scc1 binds stably to the Smc1/3 heterodimer. His$_6$Scc1, Smc1, and HA$_3$Smc3 were coexpressed in insect cells and purified over Ni^{2+}-NTA and gel filtration. No major bands besides the three cohesin subunits were detected in a silver stain of the peak elution fraction, except one band (*) that was identified to consist of Hsp70 chaparone family protein by mass-spectrometry. A minor portion of Scc1 is phosphorylated (upper band of His$_6$Scc1).

(C) The Smc1 hinge domain is not necessary for Smc1 association with Scc1. Smc1Δhinge or Smc1 were coexpressed with His$_6$Scc1 and used in binding experiments to Ni^{2+}-NTA as in (A).

(D) The Smc1/3 head domains are necessary for Scc1 binding. HA$_3$Smc1 and His$_6$Smc3 or HA$_3$Smc1Δhead and Smc3Δhead His$_6$ were coexpressed with His$_6$Scc1. The wild-type or headless Smc1/3 heterodimers were pulled down by anti-HA immunoprecipitation, and coprecipita-tion of His$_6$Scc1 was probed on an anti-His immunoblot (upper panel). Effective immunoprecipitation of the Smc1/3 heterodimer is shown by probing for His$_6$Smc3(Δhead) and HA$_3$Smc1(Δhead) (middle and lower panel).

(E) The Smc3head domain is sufficient for Scc1 binding. N- and C-terminal globular domains of Smc3 were fused by a short linker to generate an isolated Smc3 head domain. His$_6$Scc1 was expressed with and without HA$_3$Smc3head domain in insect cells and subjected to anti-HA immunoprecipitation.

detectable in Smc3HA$_6$ immunoprecipates from either fraction. It was nevertheless efficiently coimmunopreci-pitated with Smc1HA$_6$ from extracts prepared from a diploid in which Smc1 (and not Smc3) was tagged with the HA$_6$ epitope. When we used diploid strains ex-pressing myc$_{18}$-tagged Smc1 plus either Smc1HA$_6$ or Smc3HA$_6$, little or no Smc1myc$_{18}$ coimmunoprecipated with Smc1HA$_6$, but Smc1myc$_{18}$ was efficiently coimmu-noprecipitated with Smc3HA$_6$ (data not shown). To ex-clude the possibility that cohesin complexes fall apart during the preparation of these extracts, we repeated

the experiment using a diploid strain expressing myc$_6$ and HA$_6$-tagged Smc3 proteins and a myc$_{18}$-tagged Scc1 protein. Scc1myc$_{18}$ but little or no Smc3myc$_6$ co-precipitated with Smc3HA$_6$ (Figure 6B). Thus, Smc3 mol-ecules coprecipitate with those of Smc1 and Scc1 (from both soluble and chromatin-released fractions) but rarely if ever with other molecules of Smc3. This sug-gests that few if any different Smc1/3 heterodimers are linked together by Scc1 in yeast, which is contrary to the proposal that Scc1 links two heterodimers, each bound to a sister chromatid (Uhlmann et al., 1999). The
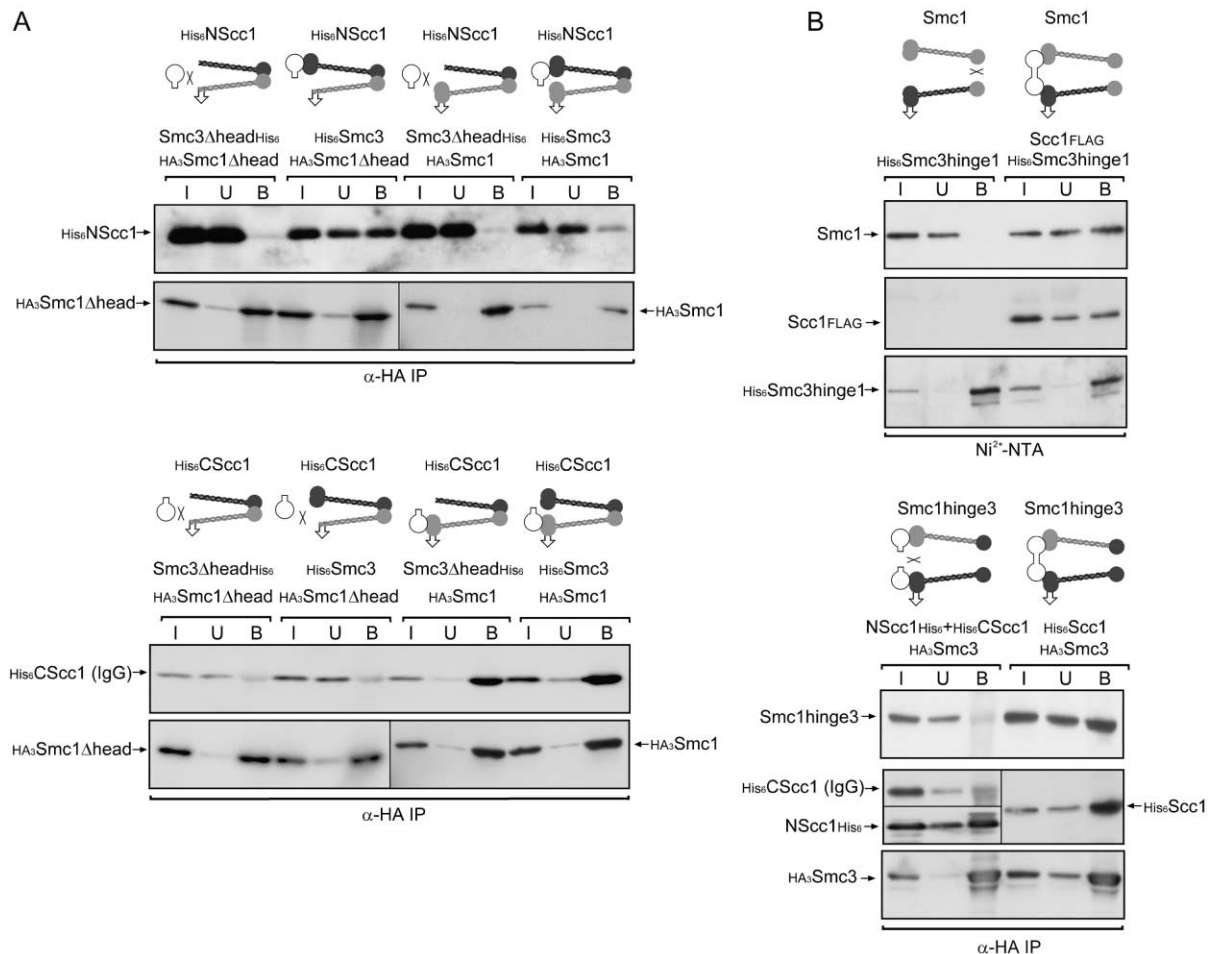
Figure 5. Scc1 Links the Head Domains of Smc1 and Smc3

(A) The Smc1 head domain binds to the C-terminal Scc1 separase cleavage fragment, the Smc3 head domain to the N-terminal fragment. Smc1/3 heterodimers lacking both head domains, lacking only the Smc1 or Smc3 head domain or wild-type heterodimers, were coexpressed with either the N-terminal or C-terminal separase cleavage fragment of Scc1 in insect cells. The heterodimer combinations were immunoprecipitated by the HA$_3$-epitope tag on Smc1 or Smc1Δhead, respectively, and coprecipitation of the His$_6$-tagged Scc1 fragments was probed by immunoblotting against the His$_6$ epitope (upper panels). The C-terminal separase cleavage fragment comigrates with the IgG heavy chain, resulting in background signals in the bound (B) fractions. The efficiency of the immunoprecipitation is shown by probing the immunoblots with anti-HA specific antibody (lower panels).

(B) Intact Scc1 can bring together Smc1 and Smc3 that have lost the ability to dimerize via their hinges. Smc1 and His$_6$Smc3hinge1 were coexpressed by themselves or together with Scc1 in insect cells (top). Protein extracts were run over a Ni^{2+}-NTA resin and eluted with imidazole. Presence of Smc1 in the fractions was followed by immunoblotting with anti-Smc1-specific antibody. Binding of His$_6$Smc3hinge1 and Scc1 to the resin was confirmed by probing with specific antibody to the FLAG epitope tag on Scc1 and to the His$_6$ epitope. Smc1hinge3 and HA$_3$Smc3 were coexpressed with both N-and C-terminal Scc1 cleavage fragments or full-length Scc1 (bottom). HA$_3$Smc3 was immunoprecipitated. Coimmunoprecipitation of Smc1hinge3 was tested by probing with Smc1-specific antibody. Full-length Scc1 and both Scc1 fragments were His$_6$ tagged, allowing detection with anti-His$_6$-specific antibody. Effective immunoprecipitation of HA$_3$Smc3 was confirmed by probing with anti-HA antibody.

corollary is that individual Scc1 molecules normally bind to the Smc1 and Smc3 heads of a single heterodimer. Scc1 is nevertheless capable of linking differently marked Smc1/3 heterodimers when these proteins are overproduced from baculoviruses in insect cells (Figure 6C), possibly because of unnaturally high protein concentrations.

Scc1 Links Scc3 to the Smc1/3 Heterodimer

To investigate how cohesin's fourth subunit, Scc3, binds to the other three constituents, we first expressed a myc$_9$ epitope-tagged Scc3 protein (myc$_9$Scc3) in insect

cells along with either full-length His$_6$-tagged Scc1 or its N- or C-terminal separase cleavage fragments. The amount of Scc3 associated with each Scc1 protein purified on Ni^{2+}-NTA was measured by Western blotting (Figure 7A). Scc3 copurified with full-length Scc1 and its C-terminal fragment but not with its N-terminal fragment. This suggests that Scc3 binds Scc1 via Scc1's C terminus. To determine whether Scc3 also binds directly to the Smc1/3 heterodimer, we coexpressed myc$_9$Scc3 together with an Smc1/3 heterodimer whose Smc3 protein was tagged with HA epitopes. Little or no myc$_9$Scc3 coprecipitated with the Smc1/3 heterodimer when im-
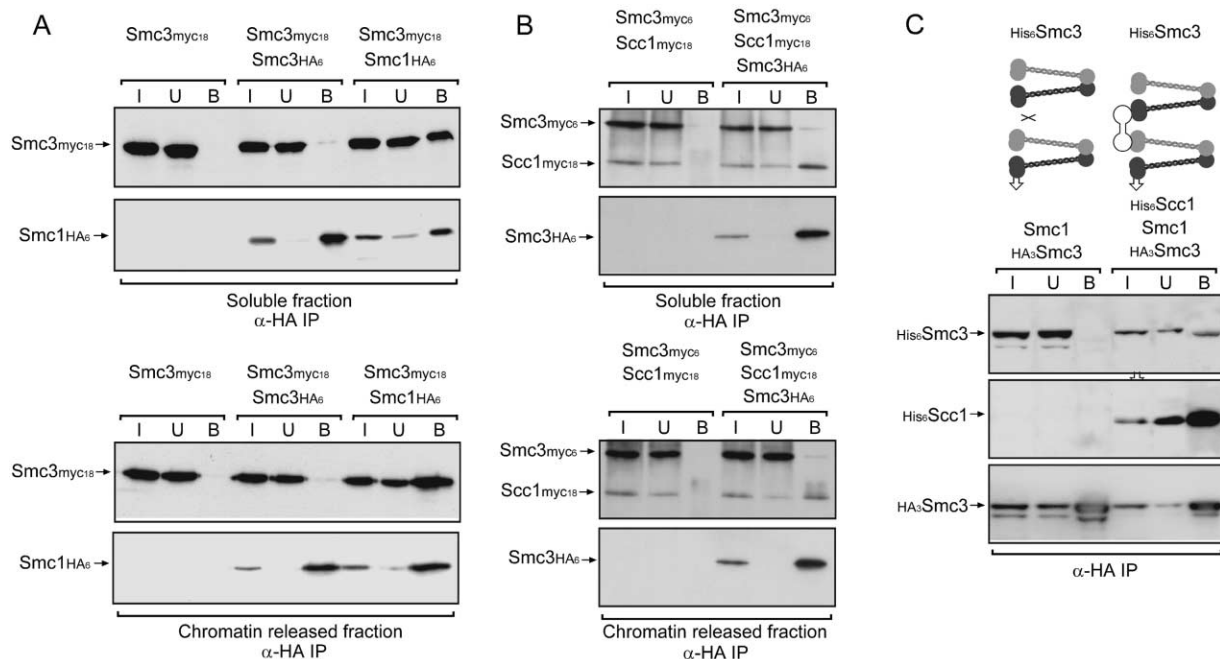
Figure 6. Only One Copy of Smc1 and Smc3 Proteins Present in Cohesin Complexes Isolated from Yeast

(A) Only one Smc3 in a single cohesin complex. Extracts were prepared from yeast strains expressing the indicated epitope-tagged versions of Smc1 or Smc3 (K6396, K10036, K10037). Soluble extracts were separated from chromatin, and cohesin complexes were released from chromatin by micrococcal nuclease digestion. Soluble and chromatin-released extract fractions were used in immunoprecipitation experiments against the HA$_6$ epitope tag, and coimmunoprecipitation of myc$_{18}$-tagged proteins was probed with anti-myc-specific antibodies in immunoblots (upper panels). Efficient immunoprecipitation of HA-tagged Smc1 and Smc3 proteins was confirmed by probing with anti-HA antibodies (lower panels).

(B) Scc1 is associated with immunoprecipitated Smc3. As in (A), using strains expressing the indicated tagged Smc3 and Scc1 versions (K10039, K10038).

(C) Scc1 is capable of binding two different Smc1/3 heterodimers when overexpressed in insect cells. Smc1 together with His$_6$- and HA$_3$-tagged versions of Smc3 were coexpressed in insect cells with and without His$_6$Scc1. After immunoprecipitation of Smc1/3 heterodimers containing HA$_3$Smc3, coprecipitation of His$_6$Smc3 containing heterodimers was probed by immunoblotting with His$_6$-specific antibody (upper panel). HA$_3$Smc3 and His$_6$Scc1 were efficiently immunoprecipitated (middle and lower panel).

munoprecipitated via Smc3's HA$_3$ tag, but much more did so when Scc1 was expressed in the same cells (Figure 7B). A similar result was obtained when the experiment was performed using Smc1-specific antibodies to immunoprecipitate the Smc1/3 dimer (data not shown). These data suggest that Scc3 does not directly bind the Smc1/3 heterodimer but is linked to it by Scc1.

Cohesin Contains Only a Single Molecule of Scc1 and Scc3

To address whether the cohesin complex contains one or more Scc3 subunits, we coexpressed myc$_9$-tagged Scc3 along with a Scc3 version tagged with ten histidine residues (His$_{10}$) in insect cells. His$_{10}$Scc3 and myc$_9$Scc3 copurified neither when Scc3 was immunoprecipitated using myc-specific antibodies nor when His$_{10}$Scc3 was bound to Ni^{2+}-NTA (data not shown). Copurification was undetectable even when His$_{10}$Scc3 and myc$_9$Scc3 were coexpressed along with Scc1, Smc1, and Smc3. Likewise, a His$_6$-tagged version of Scc1 failed to copurify with a FLAG-tagged version of Scc1 fused to a chitin binding domain (data not shown). Thus, neither Scc1 nor Scc3 bind to themselves when overexpressed in insect cells.

These data suggest that cohesin contains only a single molecule of Scc3. To verify this, we created a diploid

yeast strain that expressed Scc1myc$_{18}$, Scc3myc$_{18}$ from one allele and Scc3HA$_3$ from the other. Scc1myc$_{18}$ but not Scc3myc$_{18}$ coprecipitated with Scc3HA$_3$ from soluble and chromatin-released extracts (Figure 7C). This confirms that there is only a single Scc3 molecule in each yeast cohesin complex. It also implies that the same must be true for Scc1, because it binds directly to Scc3. To test this directly, we repeated the above experiment using a yeast strain expressing Scc1myc$_{18}$ and Scc1HA$_6$ as well as Scc3myc$_{18}$. As expected, Scc3myc$_{18}$ but not Scc1myc$_{18}$ coimmunoprecipitated with Scc1HA$_6$ (Figure 7C). The fact that all tagged proteins are functional in vivo (Toth et al., 1999) and that Scc1myc$_{18}$ and Scc3myc$_{18}$ coprecipitate with Scc3HA$_6$ and Scc1HA$_6$, respectively, implies that all these epitope-tagged proteins are indeed assembled into cohesin complexes. Our data suggest that cohesin contains only a single molecule each of Scc1 and Scc3.

Discussion

Both Eukaryotic and Prokaryotic SMC Proteins Form Intramolecular Coiled Coils

Studies of bacterial SMC proteins (Löwe et al., 2001; Melby et al., 1998) have hitherto failed to determine whether their arms are composed of inter- or intramolec-
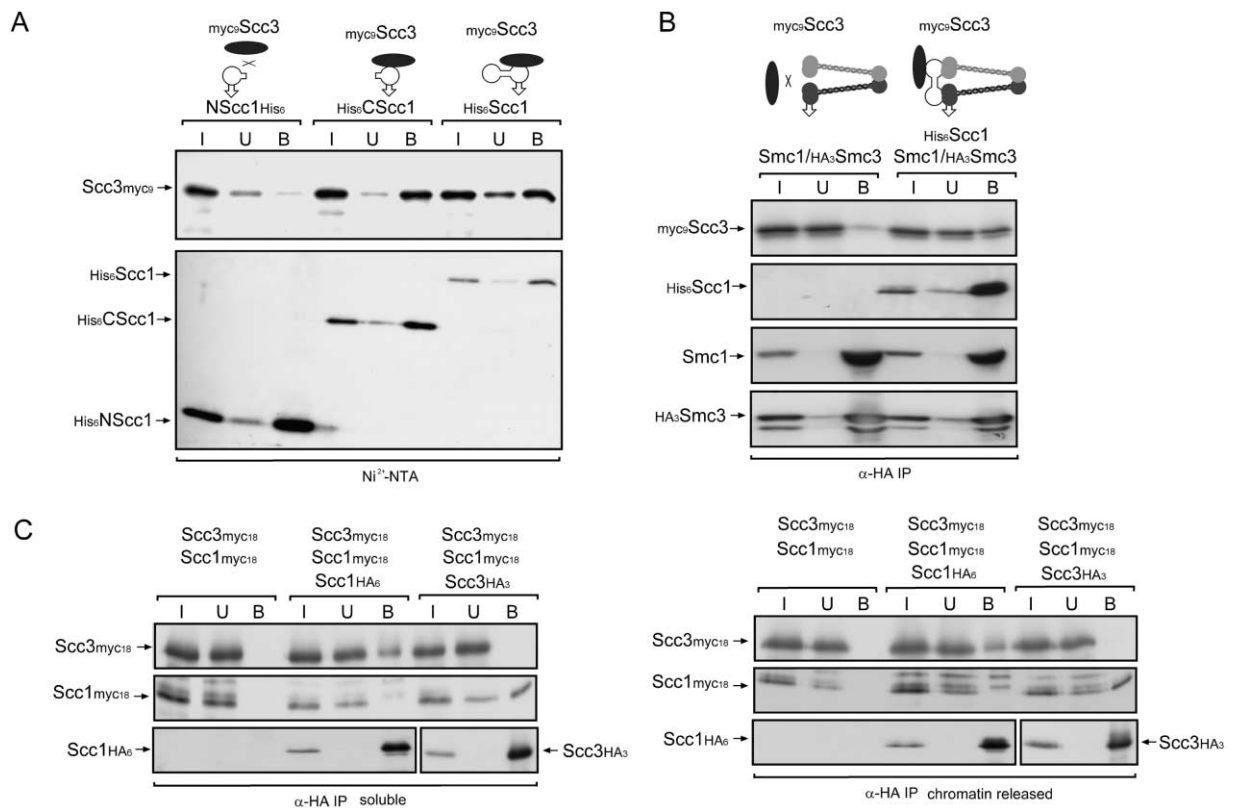
Figure 7. Scc1 Bridges a Single Scc3 to the Smc1/3 Heterodimer

(A) Scc3 only binds to the C-terminal separase cleavage fragment of Scc1. Myc$_9$Scc3 was coexpressed with His$_6$-tagged versions of full-length, N- or C-terminal separase cleavage fragments of Scc1 in insect cells. Protein extracts were run over Ni^{2+}-NTA and copurification of myc$_9$Scc3 was followed by immunoblotting against the myc$_9$ epitope (upper panel). Binding of all Scc1 versions to the Ni^{2+}-NTA resin was confirmed by probing with anti-His$_6$-specific antibody (lower panel).

(B) Scc1 is necessary to link Scc3 to the Smc1/3 heterodimer. Myc$_9$Scc3, Smc1, and HA$_3$Smc3 were coexpressed with and without His$_6$Scc1 in insect cells. The Smc1/3 heterodimer was immunoprecipitated with anti-HA-specific antibody and coprecipitation of myc$_9$Scc3 was assayed by immunoblotting with anti-myc-specific antibody (upper panel). Efficient immunoprecipitation of the Smc1/3 (and Scc1) proteins was detected with specific antibodies (middle and lower panels).

(C) Only one copy of Scc1 and Scc3 present in yeast cohesin complexes. Soluble and chromatin-released extracts from yeast strains expressing the indicated epitope-tagged versions of Scc1 or Scc3 (K10128, K10129, K10130) were used in immunoprecipitation experiments against the HA$_6$ epitope tag, and coimmunoprecipitation of myc$_{18}$-tagged proteins was probed with anti-myc-specific antibodies in immunoblots (upper panels). Scc1HA$_6$ and Scc3HA$_6$ were completely immunoprecipitated (lower panels).

ular coiled coils. Because eukaryotic SMCs are thought to form heterodimers, the arrangement of their coiled coils has a crucial bearing on the composition of their heads, that is, whether they are composed of N and C termini from the same or different SMC protein. Reasoning that all SMCs would use the same arrangement and that the structure of any one hinge domain might reveal the exit path of their coiled coils, we determined the crystal structure of the hinge domain of SMC from the bacterium *T. maritima*. The structure showed that isolated hinges form doughnut-shaped dimers and that both N and C termini emerge from the same face, which explains why the coiled coil arms of SMC proteins form open or closed V shapes but did not reveal whether the termini seed intra- or intermolecular coiled coil formation.

Though no ordered coiled coils were visible in our first *T. maritima* hinge structure, biochemical analysis of Smc1 and Smc3 strongly suggests that these SMC proteins form intramolecular coiled coils. Smc1 and Smc3 exist as monomers when expressed alone in in-

sect cells but when coexpressed exist as 1:1 heterodimers, whose appearance under the electron microscope resembles that of *B. subtilis* SMC homodimers. Electron microscopy of Smc3 molecules on their own showed that they exist as rods with a small globular domain at one end and a larger one at the other. The latter must be jointly composed of its N- and C-terminal domains because their replacement by fibronectin repeats gives rise to a pair of short thick rods instead. Remarkably, replacement of Smc3's hinge domain by that of Smc1 results in an Smc3 chimera that forms a heterodimer with wild-type Smc3 resembling that normally formed between Smc1 and Smc3. These data suggest that the Smc1/3 heterodimer is formed by heterotypic interactions solely between the hinges of Smc1 and Smc3 and that each arm is composed of coiled coils created by folding back each molecule on itself, with its hinge as the folding axis. As predicted by this model, an isolated hinge from Smc3 binds to Smc1 almost as tightly as the intact molecule.

With these insights, we revisited the geometry of *T.*

maritima's hinge and solved the crystal structure of a longer hinge segment, whose ordered coiled coils clearly revealed them to be intramolecular. Because SMC proteins are presumably descended from an ancestral bacterial protein, we suggest that all proteins of this family form intramolecular coils and are joined together by homotypic (prokaryotes) or heterotypic (eukaryotes) interactions solely between their hinge domains. The finding that mutation of conserved glycine residues within the hinge domain of *B. subtilis* SMC proteins causes them to accumulate as monomers resembling those of Smc1 or Smc3 when expressed without the other (Hirano et al., 2001) is consistent with this notion. These glycines are situated in the dimer interaction surface and their mutation would be expected to disrupt hinge dimerization. Intramolecular coiled coils may also be the rule for more distant relatives of the SMC family such as Rad50 (de Jager et al., 2001), which lack globular hinge domains to form stable dimers. Formation of intramolecular coiled coils is furthermore far easier to envisage in terms of protein folding than the intermolecular ones initially proposed for SMC proteins.

Scc1 Binds to the Heads of Smc1 and Smc3

Our discovery that the Smc1/3 heterodimer has in all likelihood one arm composed of Smc1 and another of Smc3 turned out to be crucial in understanding how it interacts with cohesin's other subunits. Of these, only its cleavable Scc1 subunit binds directly to the Smc1/3 heterodimer. Scc1 also binds directly to Scc3 and thereby links this subunit to the Smc1/3 heterodimer. It is presumably no coincidence that it is cleavage of this central subunit that triggers loss of sister chromatid cohesion at the metaphase to anaphase transition (Hauf et al., 2001; Uhlmann et al., 1999).

Several lines of evidence suggest that Scc1's N-terminal half binds to Smc3's head whereas its C-terminal half binds to that of Smc1. Intact Scc1 binds to Smc1/3 heterodimers lacking either Smc1's head or that of Smc3 but not both, whereas its N-terminal fragment binds to heterodimers lacking Smc1's but not Smc3's head, and Scc1's C-terminal fragment binds to heterodimers lacking Smc3's but not Smc1's head. Scc1 cannot itself dimerize, but because it has two separate binding sites for Smc1 and Smc3 it is capable of linking the heads of these two proteins together even when they are prevented from interacting via their hinges. These observations raise the possibility that the two arms of the Smc1/3 heterodimer are linked not only through interaction between their hinges but also by the binding of their heads to different ends of a single Scc1 molecule. When and if this occurs, cohesin would form a closed proteinaceous loop (Figure 8A). Whether cohesin actually forms such loops when it binds to chromosomes and participates in sister chromatid cohesion is clearly an important question for future experiments. The recent finding that non-SMC material associated with soluble cohesin from either *Xenopus* oocyte or human cell extracts is found in the vicinity of cohesin's Smc1/3 heads (Anderson et al., 2002) is clearly consistent with our proposal that Scc1 links the heads together and with the finding that Scc3 binds exclusively to Scc1.

The non-SMC material near cohesin's SMC heads in electron micrographs in all likelihood corresponds to Scc1 and Scc3. Our failure to detect copurification of differently tagged versions of either Scc1, Scc3, Smc1, or Smc3 in soluble and chromatin released cohesin complexes (when expressed in the same yeast cell) suggests the presence of only a single molecule of these four subunits in one cohesin complex. This is in agreement with the findings that the two isoforms of Scc3 in vertebrates, SA1 and SA2, never copurify in one cohesin complex (Sumara et al., 2000) and that endogenous Scc1 protein cannot be coimmunoprecipitated with a myc-tagged Scc1 from human cell extracts (S. Hauf and J.M. Peters, personal communication). If Scc1 links the heads of Smc1 and Smc3 together, then it appears to link only heads from Smc1 and Smc3 also held together at their hinges.

A Model for Sister Chromatid Cohesion

There have been several proposals for how cohesin might connect sister chromatids. According to one, sisters are joined by a single Smc1/3 heterodimer, one of whose heads binds one DNA molecule while the other binds its sister (Toth et al., 1999; Losada and Hirano, 2001; Anderson et al., 2002). According to this model, the gap between sister chromatids is spanned by the heterodimer's hinge and coiled regions. The binding of one or both heads is presumably facilitated by cohesin's cleavable Scc1 subunit. Our failure to find more than one molecule of Scc1 associated with the Smc1/3 heterodimer means that any bridge of this nature would have to be asymmetric with only one of the two SMC-DNA connections involving Scc1. A variation on this theme would have two different heterodimers cooperate in creating the bridge between sisters. One chromatin fiber could be bound by an Smc1 head from one heterodimer linked by Scc1 to the Smc3 head from a second one whereas its sister would be bound by the Smc3 head from the first heterodimer linked by a second Scc1 molecule to the Smc1 head from the second (Anderson et al., 2002). This model is inconsistent with our finding that both soluble and chromatin released cohesin contain only a single Smc1/3 heterodimer and only a single molecule of Scc1 and Scc3. However, we cannot exclude the possibility that cohesin does indeed form multimers when bound to chromatin, but that these higher order complexes are disrupted by nuclease digestion. According to yet another model, an Smc1/3 heterodimer, which is bound to one DNA molecule via both of its heads, is connected with the help of Scc1 to a second heterodimer bound to its sister (Losada and Hirano, 2001; Uhlmann et al., 1999). This model predicts that Scc1 would bind either to the Smc1/3's hinge or coiled coils. Our finding that Scc1 has little or no affinity for Smc1/3 heterodimers lacking their heads shows that this is not the case.

Our results showing that Scc1 links the two heads of a single Smc1/3 heterodimer, thereby creating a huge proteinaceous loop or ring, raises yet a third possibility, namely that sister chromatids are held together through their entrapment by a single closed cohesin loop. According to this model, destruction of cohesion by separase is not due to any radical change in the chemistry
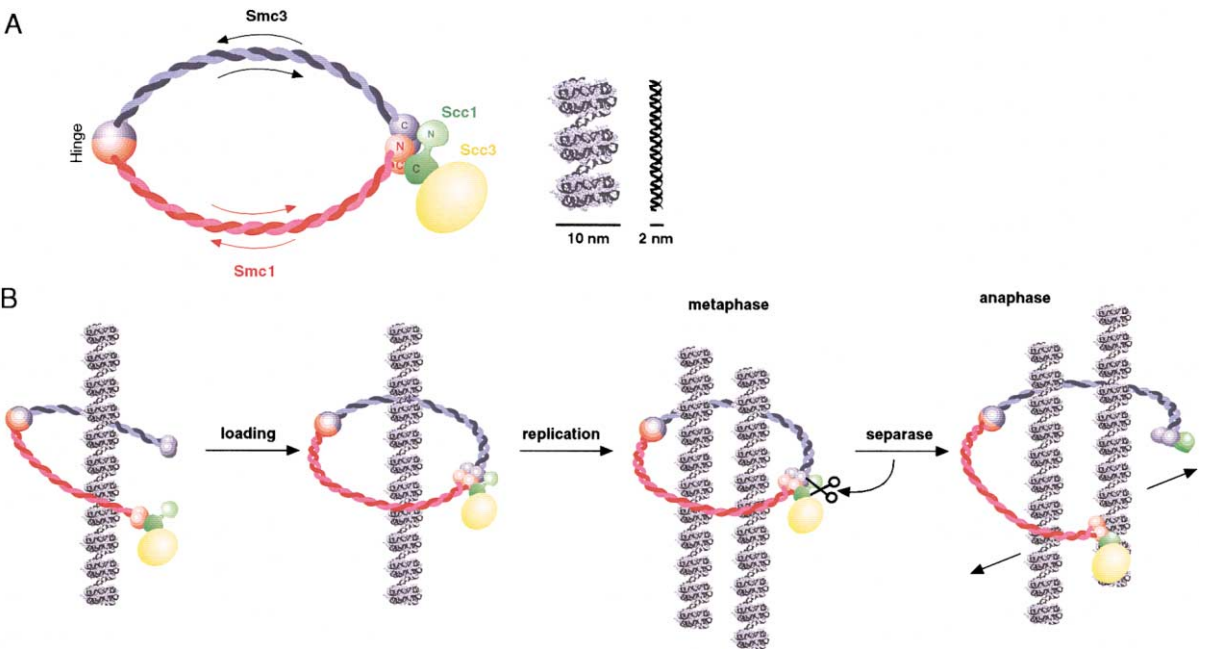
Figure 8. Model of the Yeast Cohesin Complex

(A) Smc1 and Smc3 form a heterodimer with intramolecular coiled coils. Scc1 bridges the head domains of Smc1 and Smc3 and links them to Scc3. For comparison, a schematic 10 nm chromatin fiber of DNA wrapped around nucleosomes and a DNA double helix are shown in scale to the Smc1/3 ring.

(B) Hypothetical "embrace" model of how the cohesin complex might confer sister chromatid cohesion. Before the commencement of replication, the cohesin complex is loaded onto DNA. The arms of the Smc1/3 molecules embrace the DNA, thereby forming a ring of approx. 40 nm diameter. The head domains of Smc1 and Smc3 are locked together by Scc1. Now, cohesion might be generated as the replication fork passes through the ring, entrapping both sister chromatids inside. At the metaphase to anaphase transition, Scc1 is cleaved by separase, thereby opening the lock of the Smc1/3 head domains. The ring opens and sister chromatids can be pulled to opposite spindle poles.

of cohesin's interaction with DNA but is simply due to breakage of the chromatin fiber's topological enclosure. By supposing that cohesin associates with unreplicated chromatin in a similar if not identical manner, this "embrace" model explains how cohesin can be so tightly associated with chromatin throughout interphase with-

out having a high natural affinity for DNA. It also provides an explanation for the perplexing issue as to how cells ensure that sister DNA molecules but not others are held in cohesin's embrace, why cohesin must be present during DNA replication (Uhlmann and Nasmyth, 1998), and why SMC proteins contain unusually long coiled coil

Table 1. Refinement Statistics

	P2$_1$	P2$_1$2$_1$2$_1$	C2
residues	chain A: 498–658	chain A: 501–658	chain A: 475–679
	chain B: 496–657	chain B: 497–657	chain B: 475–679
		chain C: 501–658	chain C: 475–679
		chain D: 501–656	chain D: 482–679
water molecules	174	no water built	no waters built
resolution	2.0 Å	3.0 Å	3.0 Å
twinning fraction[a]	not twinned	0.158 (k, h, -l)	not twinned
R-factor, R-free[b]	0.226, 0.267	0.253, 0.298	0.252, 0.301
B average[c]	45.7 Å^2	49.68 Å^2	84.9 Å^2
Geometry[d]	0.005 Å, 1.135°	0.009 Å, 1.332°	0.009 Å, 1.363°
Ramachandran[e]	91.4%/0.0%	78.9%/0.2%	76.4%/1.1%
NCS RMS[f]	no NCS restraints	0.11 Å (average)	0.06 Å (average)
PDB ID[g]	1GXJ	1GXK	1GXL

[a] Twinning fraction as used in refinement, operator -h, -k, l.
[b] 5% of reflections were randomly selected for determination of the free R factor (keeping twin-related reflections together), prior to any refinement.
[c] Temperature factors averaged for all atoms.
[d] RMS deviations from ideal geometry for bond lengths and restraint angles.
[e] Percentage of residues in the "most favoured region" of the Ramachandran plot and percentage of outliers (PROCHECK).
[f] RMS deviation of symmetry related atoms. Tight NCS restraints were used for the low-resolution structures.
[g] Protein Data Bank identifers for coordinates.

segments. Cohesion between sisters could conceivably be established by replicating through a preexisting cohesin loop that had previously embraced the unreplicated DNA (Figure 8B). With a diameter of ∼40 nm, cohesin's loop should be large enough to permit passage of a replisome. However, such a feat would be hard to imagine if the diverging forks from a single replicon were held together, as has been suggested in bacteria (Lemon and Grossman, 2000). It is therefore possible that loops that end up embracing sister chromatids are only generated in the replisome's wake.

If correct, the embrace model raises important questions as to how cohesin's arms open and shut during its loading onto chromatin. If soluble cohesin is also in a closed form, then it must open before it can embrace a DNA molecule and reclose around it. Several of cohesin's properties may be pertinent to this issue. The first is the potential ATPase activity of its two heads, which could help to drive the embracing process. The second is the finding that cohesin's association with yeast chromatin depends on a second complex containing the Scc2 and Scc4 proteins, which interact only very loosely with cohesin (Ciosk et al., 2000) and might regulate opening and closing. A third concerns the roles of Scc3 and Pds5, which are clearly not required for the formation of closed loops but could easily regulate their opening and/or persistence.

In conclusion, our finding that cohesin has separate Smc1 and Smc3 arms that can be joined by its cleavable Scc1 subunit suggests a novel hypothesis for how sister chromatids are held together after DNA replication. The model's attractions are not the weight of data behind it, which is only modest so far, but rather its explanatory power. It makes a number of testable predictions, not least of which is that cohesion should depend on the integrity of all components of the proposed loop. It is not inconceivable that a protein-DNA intercatenation principle lies behind the function of other SMC protein complexes.

Experimental Procedures

Thermotoga maritima SMC Hinge Domain Crystal Structures

The hinge domain part of SMC (HTMC) from *Thermotoga maritima* (DSMZ number 3109; TmSMC: TM1182 [SWALL: Q9X0R4]) was amplified by genomic PCR and expressed in *E. coli*. C41 (Miroux and Walker, 1996) as C-terminal His$_6$-tag fusions. Two constructs were used in this study: HTMC2 (coding for residues 485-670) and HTMC9 (coding for residues 473-685). Native and Seleno-methionine (SeMet) substituted proteins were produced using NiNTA resin following published procedures (van den Ent et al., 1999). HTMC9-expressing cells were lysed after powdering under liquid nitrogen in a mortar by boiling for 90 s to overcome proteolysis problems. All crystals were grown by sitting drop vapor diffusion at 19°C. Monoclinic (P2$_1$) native crystals of HTMC2 were grown using 26% PEG 3000 and 0.1 M CHES (pH 9.2) as crystallization solution. Drops were composed of 2 μl protein at 20 mg/ml and 1 μl crystallization solution. SeMet substituted HTMC2 crystals were grown in the same manner as for the native protein but at 10 mg/ml with 30% PEG 3000 and 0.1 M CHES (pH 9.2). Orthorhombic crystals of HTMC2 (P2$_1$2$_1$2$_1$) were grown using 15% PEG 2000MME and 0.1 M TRIS (pH 6.9) as the crystallization solution. Drops were composed of 3 μl protein at 10 mg/ml and 1 μl crystallization solution. All HTMC2 crystals were frozen in mother liquor complemented with 8%–12% glycerol. SeMet HTMC9 protein crystallized in C2 using 0.1 M sodium citrate, 0.1 M sodium cacodylate, and 30% iso-propanol as crystallization solution. Crystals were frozen in crystallization solution with 10% isopropanol added.

Diffraction data were collected on beamline 14-1 and 9.5 (SRS, Daresbury, UK) and 14-4 (ESRF, Grenoble, France). Crystal data and dataset and refinement statistics are summarized in Table 1 and Supplemental Table S1 at http://www.molecule.org/cgi/content/full/9/4/773/DC1. Crystals were indexed and integrated using MOSFLM (CCP4) and data were further processed using the CCP4 package (CCP4, 1994). An initial 2.5 Å MAD density map of crystal form P2$_1$ was obtained using the program SOLVE (Terwilliger and Berendzen, 1999), which was also used to calculate phases. After solvent flattening, all ordered residues were built into the MAD electron density map using MAIN2001 (Turk, 1992). The structure was refined against all data in dataset P2$_1$ to 2.0 Å resolution using CNS (Brünger et al., 1998). The structure of the SMC hinge domain dimer in the P2$_1$ crystals appeared to be distorted by crystal packing. Dataset P2$_1$2$_1$2$_1$ showed significant twinning when comparing cumulative intensity distributions to those from randomly scattered atoms (TRUNCATE, CCP4). The twinning is a rotation around the c axis (k, h, -l) facilitated in spacegroup P2$_1$2$_1$2$_1$ by the similarity of the a and b axis. Dataset P2$_1$2$_1$2$_1$ was solved by molecular replacement using the refined P2$_1$ model and CNS, producing only weak solutions. Torsion angle simulated annealing on several solutions picked out the correct one and facilitated a large conformational change in the model that is necessary to convert the P2$_1$ to the P2$_1$2$_1$2$_1$ crystal form. Both crystal forms contained no coiled coil segments—the residues with coiled coil prediction are largely disordered. The longer construct HTMC9 in crystal form C2 was solved by molecular replacement using the undistorted P2$_1$2$_1$2$_1$ model. To verify the initial finding of coiled coil segments in difference densities, and to have an independent indicator of the correctness of the coiled coil arrangement in the model building process, methionine positions and phases were derived from SeMet HTMC9 crystals. Selenium atoms were located using model phases and three strong peaks were detectable on the coiled coil segments. These indicated the positions of M488 and M493 of the N-terminal helix of the coiled coil. The other peak indicated the position of M678 on the C-terminal helix. Phases were calculated from the two HTMC9 SeMet datasets taking the selenium sites as above and were used for refinement and difference electron densities. The C2 datasets have high internal B factors of about 90 Å^2 (as derived from Wilson plots) that are reflected in the average B factors of the model. Coordinates and structure factors have been deposited in the Protein Data Bank (Table 1).

Baculovirus Expression Vectors

DNA sequences encoding *S. cerevisiae* genes *SMC1*, *SMC3*, *SCC1*, or *SCC3* were cloned from genomic library plasmids (Michaelis et al., 1997) into Bac-to-Bac (Gibco Life Technologies) pFASTBAC (pFB) baculovirus expression vectors. Epitope tags as described in the individual experiments were introduced at the N or C terminus of the respective coding sequence, indicated by the position of the tag name. For detailed descriptions of the constructs, see Supplemental Experimental Procedures at http://www.molecule.org/cgi/content/full/9/4/773/DC1

Expression of Yeast Proteins in Insect Cells

Recombinant baculoviruses were obtained by transposition of the expression vectors into DH10BAC cells, bacmid preparation, and transfection into Sf9 insect cells (Gibco Life Technologies). Expression of the recombinant proteins was checked by immunoblotting of lysates from transfected cells, and baculoviruses were amplified three times in Sf9 cells to obtain high viral titer stocks in the range of 5 × 10^8 to 1 × 10^9 pfu/ml. For protein expression, High Five (Invitrogen) insect cells grown at 27°C in Grace's insect media supplemented with 10% fetal calf serum, penicillin, streptomycin, and glutamine to near confluency were infected at a multiplicity of infection (MOI) of ∼10 for each high-titer virus. Cells were harvested 45 hr postinfection and extracts were prepared: cells were washed in ice-cold PBS and broken by hypotonic lysis in a Dounce homogenizer after 10 min swelling in two pellet volumes 50 mM TRIS-HCl (pH 8.0) and 10 mM KCl containing complete proteinase inhibitor mix EDTA-free (Roche Mol. Biochem.) and PMSF at 0.2 mM. Cytosolic extract was separated from nuclei by 10 min centrifugation at 5,000 × g at 4°C. Nuclei were broken after resuspension in two nuclear pellet volumes 50 mM TRIS-HCl (pH 8.0), 10 mM KCl, 1.5 mM MgCl$_2$, and proteinase inhibitor mix by increasing the NaCl

concentration in three steps to 420 mM final and vortexing after each NaCl addition. Cytosolic and nuclear extracts were cleared by subsequent 30 min high speed centrifugation steps at 40,000 × g and 100,000 × g at 4°C. Cleared cytosolic and nuclear extracts were then combined.

Gel Filtration and Glycerol Gradient Centrifugation

2 ml (resin volume) Ni^{2+}-NTA superflow (QUIAGEN) was preequilibrated in T(250/5) buffer (50 mM TRIS-HCl [pH 8.0], 10 mM KCl, 1.5 mM $MgCl_2$, first number in parentheses refers to NaCl concentration in mM, second number refers to imidazole concentration in mM). Extract prepared from ~4 × 10⁸ infected insect cells (10 T250 flasks) was adjusted to a final concentration of 5 mM imidazole and incubated with the preequilibrated Ni^{2+}-NTA resin for 3 to 4 hr shaking at 4°C. The resin was washed sequentially with 10 ml of each T(500,5), T(250,5) twice, T(100,20) and protein was eluted in three steps with 600 µl T(100,200) containing 20% glycerol. Eluates were combined.

Half of the eluate from the Ni^{2+}-NTA resin was applied onto a Sephacryl HR300 gel filtration column (Amersham-Pharmacia), using 250 mM NH_4HCO_3, 10 mM TRIS-HCl (pH 8.0), 0.2 mM EDTA, and 20% glycerol as running buffer. The column was calibrated using standard proteins (aldolase r_s = 4.8 nm, ferrtin r_s = 6.1 nm, thyroglobulin r_s = 8.5 nm). The Stokes radii for Smc3 and Smc1/3 were calculated following the method of Porath.

15%–30% linear glycerol gradients were prepared in 200 mM NH_4HCO_3 and 0.2 mM EDTA. 100 µl Ni^{2+}-NTA eluate was diluted with 100 µl 200 mM NH_4HCO_3 and 0.2 mM EDTA and layered on top of the gradient. Gradients were run for 24 hr at 38,000 rpm in an SW40Ti rotor (Beckman) and fractionated using an Isco fractionator. For calibration, standard proteins were run in parallel (bovine serum albumine 4.6 S, aldolase 7.3 S, catalase 11.3 S, ferritin 17.6 S, thyroglobulin 19 S) and the S values of Smc3 and Smc1/3 were calculated by linear regression of the values determined for the standard proteins (R^2 = 0.99). Presence and purity of Smc3 or Smc1/3 proteins in elution fractions from gel filtration and glycerol gradient centrifugation were determined by silver staining after SDS-PAGE. The native molecular weights of Smc3 and Smc1/3 were calculated using a partial specific volume of 0.725 cm³/g.

Electron Microscopy

3 µl of the peak fraction from the Sephacryl column was directly spread on a freshly cleaved 1 cm² mica using the sandwiching technique. Micas were dried in vacuum for at least 2 hr before rotary shadowing with 1–2 nm platinum/carbon at an angle of ~8° from an electron beam gun (Bal-Tec, MED 020). Replicas were stabilized with a 5 nm carbon layer, floated onto copper grids, and photographed in the electron microscope at 80 kV, 25,000× magnification.

Binding Assays of Baculovirus Expressed Proteins

Extracts were prepared from ~4×10⁷ insect cells 45 hr after coinfection with recombinant viruses as indicated. 200 µl cleared extract was diluted with 800 µl T(250,0) plus 0.2 mM PMSF. For binding assays on Ni^{2+}-NTA, diluted extracts were adjusted to 5 mM imidazole and incubated with 100 µl preequilibrated Ni^{2+}-NTA superflow resin (QUIAGEN) for 3 hr at 4°C. The Ni^{2+}-NTA resin was washed with 1 ml of each T(500,5), T(250,5) twice, T(100,20) and bound protein was eluted with 100 µl T(250,150). For coimmunoprecipitations, 5 µl 16B12 monoclonal antibody (BAbCO) was added to diluted extracts and allowed to bind to the HA-epitope for 1.5 hr shaking at 4°C before addition of 50 µl preequilibrated proteinG sepharose (Amersham-Pharmacia). After shaking at 4°C for another 2.5 hr, beads were washed 3 times in T(250,0) and bound protein was eluted by boiling in 100 µl SDS-loading buffer. Proteins were separated by SDS-PAGE and detected by immunoblotting, using a polyclonal antibody raised against the N terminus of Smc1 (a gift from C. Frei and S. Gasser, Lausanne) or monoclonal antibodies against the His_6 (Penta·His, Sigma), HA (16B12, BAbCO), FLAG (M2, Sigma), or myc-epitopes (9E10).

Binding Assays on Proteins Isolated from Yeast

All strains used were derivatives of W303 and carried a deletion of the PEP4 protease gene to reduce protein degradation during extract preparation and immunoprecipitations. Strains expressing cohesin subunits tagged C-terminally with multiple copies of either the HA- or myc-epitope from their original genomic loci were de-

scribed previously and have been shown to be functional in vivo (Michaelis et al., 1997; Toth et al., 1999). These strains were crossed to obtain diploid strains as indicated in the figures. Extracts from asynchronous yeast cultures were prepared following the protocol by Liang and Stillman (1997), with the exception that zymolyase T100 at 40 µg/ml was used for spheroblasting and Complete proteinase inhibitor mix (Roche Mol. Biochem.) and 0.2 mM PMSF replaced the proteinase inhibitors in the EB buffer. Chromatin pellets were separated from the soluble fraction and cohesin complexes were released from chromatin pellets by micrococcal nuclease treatment as published (Ciosk et al., 2000). Coimmunoprecipitations were carried out as described for baculovirus expressed proteins, with the exception that soluble and chromatin released fractions were precleared with proteinG sepharose before the addition of antibody.

BIAcore Measurements

All experiments were carried out at a flow rate of 5 µl/min using HBS plus 0.005% Surfactant P20 as running buffer. Rabbit anti-mouse Fc-γ antibody (BIAcore) was immobilized to a CM5 sensor chip surface at a concentration of 30 µg/ml in 10 mM Na-acetate (pH 5.0) using standard EDC/NHS crosslinking procedure. 12CA5 (anti-HA) was loaded as secondary antibody (followed by 10 µl 1M NaCl wash) to bind HASmc3 or HASmc3hinge from cleared insect cell extracts. Cleared extract from insect cells expressing Smc1 were floated over the loaded sensor and association and dissociation phases were recorded for 10 and 30 min, respectively. The sensor chip was regenerated with 30 mM HCl and 1 M NaCl and the experiment was repeated with a different dilution of Smc1 extract. The concentration of Smc1 in the extract was estimated by quantitative immunoblotting using purified Smc1 as standard, and extracts were diluted with uninfected insect cell extracts to obtain Smc1 concentrations from 20 to 200 nM. For all dilutions, Smc1 binding on lanes loaded only with secondary antibody was recorded and substracted from the curves to account for unspecific binding.

References

Anderson, D.E., Losada, A., Erickson, H.P., and Hirano, T. (2002). Condensin and cohesin display different arm conformations with characteristic hinge angles. J. Cell Biol. *156*, 419–424.

Brünger, A.T., Adams, P.D., Clore, G.M., DeLano, W.L., Gros, P., Grosse-Kunstleve, R.W., Jiang, J.S., Kuszewski, J., Nilges, M., Pannu, N.S., et al. (1998). Crystallography & NMR system: a new software suite for macromolecular structure determination. Acta Crystallogr. D Biol. Crystallogr. *54*, 905–921.

Buonomo, S.B., Clyne, R.K., Fuchs, J., Loidl, J., Uhlmann, F., and Nasmyth, K. (2000). Disjunction of homologous chromosomes in meiosis I depends on proteolytic cleavage of the meiotic cohesin Rec8 by separin. Cell *103*, 387–398.

Ciosk, R., Shirayama, M., Shevchenko, A., Tanaka, T., Toth, A., Shevchenko, A., and Nasmyth, K. (2000). Cohesin's binding to chromo-

somes depends on a separate complex consisting of Scc2 and Scc4 proteins. Mol. Cell *5*, 243–254.

CCP4 (Collaborative Computational Project 4) (1994). The CCP4 suite: programs for protein crystallography. Acta Crystallogr. D *50*, 760–763.

de Jager, M., van Noort, J., van Gent, D.C., Dekker, C., Kanaar, R., and Wyman, C. (2001). Human Rad50/Mre11 is a flexible complex that can tether DNA ends. Mol. Cell *8*, 1129–1135.

Hauf, S., Waizenegger, I., and Peters, J.M. (2001). Cohesin cleavage by separase required for anaphase and cytokinesis in human cells. Science *293*, 1320–1323.

Hirano, T., Kobayashi, R., and Hirano, M. (1997). Condensins, chromosome condensation protein complexes containing XCAP-C, XCAP-E, and a Xenopus homolog of the Drosophila Barren protein. Cell *89*, 511–521.

Hirano, M., Anderson, D.E., Erickson, H.P., and Hirano, T. (2001). Bimodal activation of SMC ATPase by intra- and inter-molecular interactions. EMBO J. *20*, 3238–3250.

Holm, L., and Sander, C. (1995). Dali: a network tool for protein structure comparison. Trends Biochem. Sci. *20*, 478–480.

Hopfner, K.P., Karcher, A., Shin, D.S., Craig, L., Arthur, L.M., Carney, J.P., and Tainer, J.A. (2000). Structural biology of Rad50 ATPase: ATP-driven conformational control in DNA double strand break repair and the ABC-ATPase superfamily. Cell *101*, 789–800.

Kraulis, P.J. (1991). MOLSCRIPT: a program to produce both detailed and schematic plots of protein structures. J. Appl. Crystallogr. *24*, 946–950.

Lemon, K.P., and Grossman, A.D. (2000). Movement of replicating DNA through a stationary replisome. Mol. Cell *6*, 1321–1330.

Liang, C., and Stillman, B. (1997). Persistent initiation of DNA replication and chromatin-bound MCM proteins during the cell cycle in cdc6 mutants. Genes Dev. *11*, 3375–3386.

Losada, A., and Hirano, T. (2001). Intermolecular DNA interactions stimulated by the cohesin complex in vitro. Implications for sister chromatid cohesion. Curr. Biol. *11*, 268–272.

Losada, A., Hirano, M., and Hirano, T. (1998). Identification of Xenopus SMC protein complexes required for sister chromatid cohesion. Genes Dev. *12*, 1986–1997.

Löwe, J., Cordell, S.C., and van den Ent, F. (2001). Crystal structure of the SMC head domain: an ABC ATPase with 900 residues antiparallel coiled-coil inserted. J. Mol. Biol. *306*, 25–35.

Melby, T.E., Ciampaglio, C.N., Briscoe, G., and Erickson, H.P. (1998). The symmetrical structure of structural maintainance of chromosomes (SMC) and MukB proteins: long, antiparallel coiled coils, folded at a flexible hinge. J. Cell Biol. *142*, 1595–1604.

Michaelis, C., Ciosk, R., and Nasmyth, K. (1997). Cohesins: chromosomal proteins that prevent premature separation of sister chromatids. Cell *91*, 35–45.

Miroux, B., and Walker, J.E. (1996). Over-production of proteins in *Escherichia coli*: mutant hosts that allow synthesis of some membrane proteins and globular proteins at high levels. J. Mol. Biol. *260*, 289–298.

Nasmyth, K. (2001). Disseminating the genome: joining, resolving, and separating sister chromatids during mitosis and meiosis. Annu. Rev. Genet. *35*, 673–745.

Neuwald, A.F., and Hirano, T. (2000). HEAT repeats associated with condensins, cohesins, and other complexes involved in chromosome-related functions. Genome Res. *10*, 1445–1452.

Panizza, S., Tanaka, T., Hochwagen, A., Eisenhaber, F., and Nasmyth, K. (2000). Pds5 cooperates with cohesin in maintaining sister chromatid cohesion. Curr. Biol. *10*, 1557–1564.

Pasierbek, P., Jantsch, M., Melcher, M., Schleiffer, A., Schweizer, D., and Loidl, J. (2001). A Caenorhabditis elegans cohesion protein with functions in meiotic chromosome pairing and disjunction. Genes Dev. *15*, 1349–1360.

Rao, H., Uhlmann, F., Nasmyth, K., and Varshavsky, A. (2001). Degradation of a cohesin subunit by the N-end pathway is essential for chromosome stability. Nature *410*, 955–959.

Siegel, L.M., and Monty, K.J. (1966). Determination of molecular weights and frictional ratios of proteins in impure systems by use of gel filtration and density gradient centrifugation. Application to crude preparations of sulfite and hydroxylamine reductases. Biochim. Biophys. Acta *112*, 346–362.

Sonoda, E., Matsusaka, T., Morrison, C., Vagnarelli, P., Hoshi, O., Ushiki, T., Nojima, K., Fukagawa, T., Waizenegger, I.C., Peters, J.M., et al. (2001). Scc1/Rad21/Mcd1 is required for sister chromatid cohesion and kinetochore function in vertebrate cells. Dev. Cell *1*, 759–770.

Soppa, J. (2001). Prokaryotic structural maintenance of chromosomes (SMC) proteins: distribution, phylogeny, and comparison with MukBs and additional prokaryotic and eukaryotic coiled-coil proteins. Gene *278*, 253–264.

Sumara, I., Vorlaufer, E., Gieffers, C., Peters, B.H., and Peters, J.-M. (2000). Characterization of vertebrate cohesin complexes and their regulation in prophase. J. Cell Biol. *151*, 749–762.

Terwilliger, T.C., and Berendzen, J. (1999). Automated MAD and MIR structure solution. Acta Crystallogr. D Biological Crystallogr. *55*, 849–861.

Toth, A., Ciosk, R., Uhlmann, F., Galova, M., Schleifer, A., and Nasmyth, K. (1999). Yeast Cohesin complex requires a conserved protein, Eco1p (Ctf7), to establish cohesion between sister chromatids during DNA replication. Genes Dev. *13*, 320–333.

Turk, D. (1992), Weiterentwicklung eines Programms für Molekülgrafik und Elektrondichte-Manipulation und seine Anwendung auf verschiedene Protein-Strukturaufklärungen. Ph. D. thesis, Technische Universität München.

Uhlmann, F., and Nasmyth, K. (1998). Cohesion between sister chromatids must be established during DNA replication. Curr. Biol. *8*, 1095–1101.

Uhlmann, F., Lottspeich, F., and Nasmyth, K. (1999). Sister chromatid separation at anaphase onset is promoted by cleavage of the cohesin subunit Scc1p. Nature *400*, 37–42.

Uhlmann, F., Wernic, D., Poupart, M.A., Koonin, E., and Nasmyth, K. (2000). Cleavage of cohesin by the CD clan protease separin triggers anaphase in yeast. Cell *103*, 375–386.

van den Ent, F., Lockhart, A., Kendrick-Jones, J., and Lowe, J. (1999). Crystal structure of the N-terminal domain of MukB: a protein involved in chromosome partitioning. Struct. Fold. Des. *7*, 1181–1187.

Waizenegger, I., Hauf, S., Meinke, A., and Peters, J.M. (2000). Two distinct pathways remove mammalian cohesin from chromosome arms in prophase and from centromeres in anaphase. Cell *103*, 399–410.

Accession Numbers

Structure coordinates of the Thermotoga SMC hinge domain are available from the Protein Data Bank under accession numbers 1GXJ (P2$_1$), 1GXK (P2$_1$2$_1$2$_1$), and 1GXL (C2).